VIP *Very Important Paper*
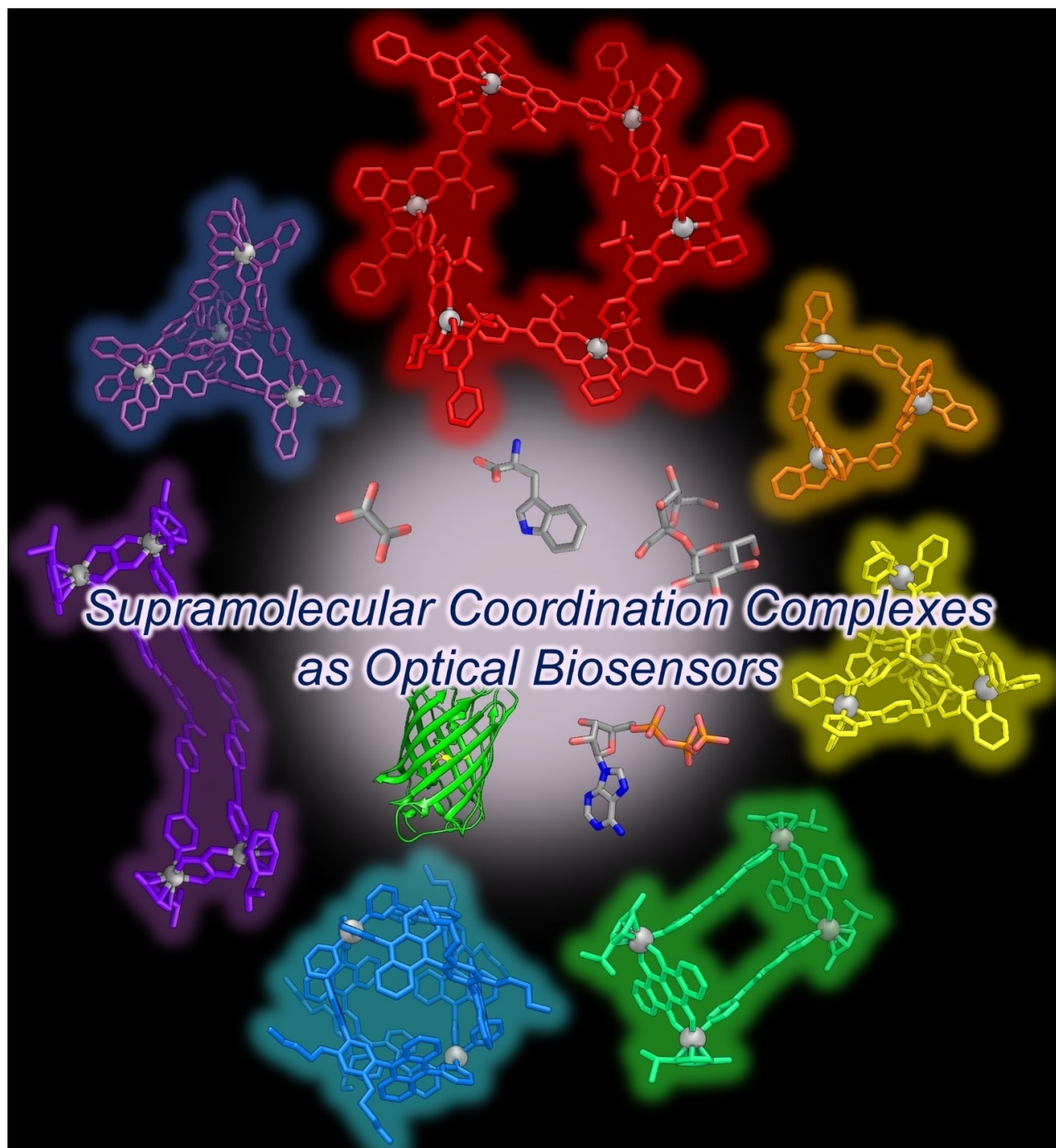
Supramolecular Coordination Complexes as Optical Biosensors

Nilanjan Dey[a] and Cally J. E. Haynes*[b]

In recent years, luminescent supramolecular coordination complexes (SCCs), including 2D-metallacycles and 3D-metallacages have been utilised for biomolecular analysis. Unlike small-molecular probes, the dimensions, size, shape, and flexibility of these complexes can easily be tuned by combining ligands designed with particular geometries, symmetries and denticity with metal ions with strong geometrical binding preferences. The well-defined cavities that result, in combination with the other non-covalent interactions that can be programmed into the ligand design, facilitate great selectivity towards guest binding. In this Review we will discuss the application of luminescent metallacycles and cages in the binding and detection of a wide range of biomolecules, such as carbohydrates, proteins, amino acids, and biogenic amines. We aim to explore the effect of the structural diversity of SCCs on the extent of biomolecular sensing, expressed in terms of sensitivity, selectivity and detection range.

1. Introduction

The coordination-driven self-assembly of well-defined, discrete 2D and 3D supramolecular coordination complexes (SCCs) has captured widespread attention. Over the years, these classes of materials have found broad applications including molecular recognition, biosensing, catalysis, and drug delivery (Figure 1).[1] Discrete metallacycles can provide an efficient platform for energy transfer and light-harvesting, since it is possible to introduce multiple functional moieties into SCCs with precise control over stoichiometry and the position of the individual functional groups.[1b] Additionally, the known anticancer activity of organometallic ruthenium and platinum complexes has prompted the development of therapeutic SCCs including these metals centres for advanced biomedical applications.[2]

The advantages of using SCCs in biological applications include: (1) the ease of fine tuning the dimensions of complexes; (2) the potential to select metal ions with specific size, coordination geometries, oxidation state and versatility for biological applications; (3) the ease of incorporating essential functional groups into the SCC scaffold through modular pre- or post-self-assembly modifications, and; (4) the guest binding potential of the internal cavities of SCCs. The selective guest-binding capacity of SCCs derives from their well-defined internal cavities and drives interest into their application for analyte discrimination and sensing.[1b,3] In particular, the development of SCCs with a fluorescence signature provides a route towards an optical readout upon guest capture. Fluorescent SCCs can be developed through selection of metals (Zn^{2+}, Tb^{3+}, Fe^{3+}, etc) and/ or organic ligands with intrinsically fluorescent properties.

The use of 2D-metallacycles and 3D-metallacages are advantageous for biomolecular analysis because of their biomimetic character and ease of synthesis via self-assembly routes.[4] Conventional fluorophores often experience aggregation-induced quenching due to intermolecular interactions, which will decay or relax the excited state back to the ground state via nonradiative pathways.[5] However, with selection of proper functional groups and fluorophore units via pre- and post-assembly modifications, SCCs often show high quantum efficiency both in the solution and solid state (an aggregated state).[6] Moreover, SCCs have been found to be soluble in water due to their highly-charged structure owing to multiple metal ion centers,[7] yet can be adapted to be soluble in lipid membranes through the use of lipophilic ligands.[8] Additionally, the large-size and high-molecular-weight of multinuclear metal complexes mean that they can selectively enter and remain in tumour cells over normal cells via the enhanced permeability and retention effect.[1d,9] Recently, Lusby (B. P. Burke, W. Grantham, M. J. Burke, G. S. Nichol, D. Roberts, I. Renard, R. Hargreaves, C. Cawthorne, S. J. Archibald, P. J. Lusby, *J. Am. Chem. Soc.* **2018**, *140*, 16877–16881) and Casini[10] have reported biocompatible supramolecular metallacages that can carry a radioactive $^{99m}TcO_4^-$ anion and be effectively applied for *in vivo* imaging.

Biological studies, such as cell-imaging and drug delivery have been widely conducted involving SCCs due to their
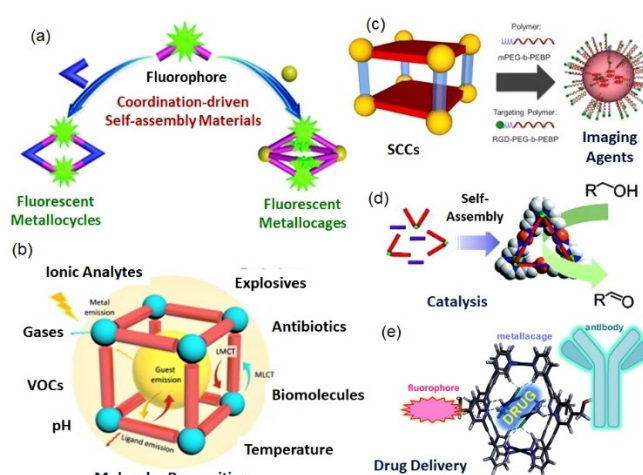
[a] Dr. N. Dey
Graduate School of Science
Kyoto University (Japan)

[b] Dr. C. J. E. Haynes
Department of Chemistry
University College (London)
E-mail: cally.haynes@ucl.ac.uk

This article is part of a Special Collection on "Supramolecular Chemistry: Young Talents and their Mentors". More articles can be found under https://onlinelibrary.wiley.com/doi/toc/10.1002/(ISSN)2192-6506.Supramolecular-Chemistry.

Figure 1. (a) Schematic diagram shows formation of 2D-(metallacycles) and 3D-(metallacages) SCCs. Applications of SCCs in (b) molecular recognition, (c) bioimaging, (d) catalysis, and (e) drug delivery. (a, c, d, e) reproduced from [1b,c,e,16] with permission from the Royal Society of Chemistry, Elsevier and the American Chemical Society. (e) reproduced from [1d].

attractive structural features.[1b,11] For example, the introduction of functional units such as tetraphenylethene (TPE) into metallacycles or cages can improve the precision of cell imaging and achieving "tissue-specific" aggregation and imaging.[12] Similarly, Stang *et al.* have developed porphyrin-based metallacages in which the careful selection of the metal ions in the porphyrin rings enabled multimodal three-state imaging with magnetic resonance imaging (MRI), positron emission tomography (PET), and near-infrared fluorescence imaging (NIRFI).[13] Researchers including Crowley[14] and Casini[15] have developed metallacapsules which can be used as carriers for target-specific loading and releasing drug molecules such as cisplatin. However, in the present review article we will focus on the application of luminescent SCCs in biomolecular sensing, and examine the context of structural diversity on these sensing applications.

2. Tuning the photophysical properties of SCCs

The photophysical properties of metallacycles and cages are highly diverse. Even small variations in the ligand design can yield substantial changes to the shape, size or flexibility of the complexes formed, which can in turn lead to changes in their optical properties. In this context, the role of the bite angle, substituents, shape and size of supramolecular coordination complexes as well as the counter anions on fluorescence properties of SCCs have been investigated.

Stang and co-workers have reported that the size of metallacycles (more precisely the bite angle) can dictate the extent of excited-state planarization of the core, which consequently alters their photophysical properties,[17] and that the fluorescence properties of the metallacycles are also influenced by their shape. They have reported the synthesis of the tetraphenylethylene (TPE)-based metallarhomboid (1) and triangle (2) by carefully controlling the shape and stoichiometry of the building blocks (Figure 2(a)).[18] Though the metallarhomboid 1 exhibited weaker fluorescence in dilute solution when compared to the triangular metallacycle 2, the reverse situation was observed in the aggregated state. The authors concluded that variation in the stability and rigidity of the assemblies resulted in their different fluorescence responses.
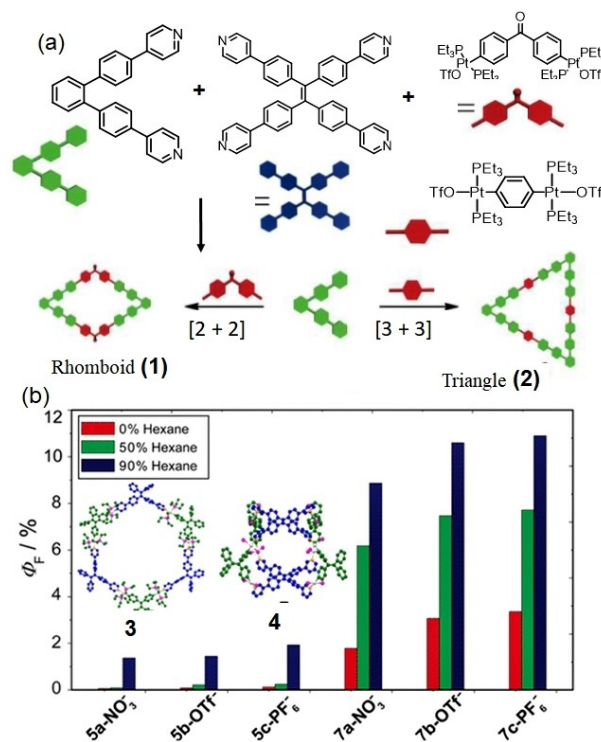

Figure 2. (a) The structure of supramolecular coordination complexes **1–2**; (b) the effect of structural variation on the fluorescence properties of supramolecular coordination complexes **3–4**. Reproduced from references [18] and [19] with permission from the American Chemical Society.

The counteranion chosen to balance the charge of cationic SCCs can play a large role in the formation of aggregate species and can therefore be influential in determining the optical properties of the assembly. Stang and co-workers have also reported tetraphenylethylene (TPE)-based drum-shaped metallacycles (**3**, **4**) and investigated the influence of the counter-anion on the photophysical properties of their assemblies (aggregation-induced-emission) (Figure 2(b)).[19] The molar absorption coefficients (ε), fluorescence emission intensities, and quantum yield (Φ_F) values in CH_2Cl_2 follow the order $PF_6^- > OTf^- > NO_3^-$. The effect of counter ion on fluorescence properties of SCCs was explained by Hofmeister
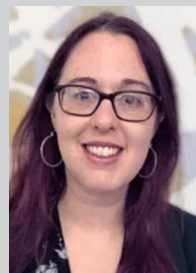
Cally Haynes is a Lecturer in Organic Chemistry and Chemical Biology at University College London. She obtained her PhD in 2011 from the University of Southampton under the supervision of Prof. Phil Gale. She carried out postdoctoral work in the same group until 2013 before joining the Royal Society of Chemistry as an editor. She returned to the lab in 2015 as a postdoctoral research associate in the group of Prof. Jonathan Nitschke, and joined UCL as a lecturer in 2019. Her research interests include the development of metal-organic hosts for biological recognition and function.

Nilanjan Dey obtained his PhD from Department of Organic Chemistry, Indian Institute of Science, Bangalore in 2017 under supervision of Prof. Santanu Bhattacharya. Currently, he is working as JSPS postdoctoral fellow at Kyoto University. He is interested in developing new molecular probes for detection of biologically relevant analytes.

ChemPlusChem

Reviews
doi.org/10.1002/cplu.202100004

Chemistry Europe
European Chemical
Societies Publishing

effect wherein the nature of counterions dictate both the solubility and 3D-structures of biomacromolecules.

Substituent effects in the design of the organic ligand components of SCCs can also play a role in tuning the luminescence of the assemblies. Stang and co-workers have reported the synthesis of a wide variety of rhomboidal metallacycles via the coordination-driven self-assembly of a phenanthrene-21-crown-7-based diplatinum(II) acceptor with a 120° dipyridyl donor (**5**) (Figure 3(a)).[20] The fluorescence emission maxima of these complexes were observed to shift from 427 nm to 593 nm depending upon the substituents (triphenylamine, pyrene, tetraphenylethene) on the dipyridyl donors. The authors reasoned that the substituents could affect the stacking pattern of the metallacycles, resulting in the modulation of the emission as well as the quantum yield, leading to the generation of white luminescence in solution. Similarly, Yang *et al.* have reported nine Pt(II)-based fluorescent metallacycles with various substitutions (**6**) (Figure 3(b)).[21] The metallacycles exhibit a wide-range of fluorescence signals, with changes in fluorescence emission maxima as well as quantum yields by simply regulating their photoinduced electron transfer (PET) and intramolecular charge transfer (ICT) properties. Thus, designing SCCs with proper size and shape is not only important for effective guest binding, but also to obtain a reliable and detectable signal upon interaction with target analytes.

Finally, the "heavy metal effect" is also an important consideration in the design of luminescent SCCs. It has been shown that constructing highly fluorescent ligands (including ligands which have been exo-functionalised with a fluorophore) is not always sufficient to ensure that the resulting SCC has desirable optical properties, since coordination to coordination to heavy metals such as Pd^{2+} can cause fluorescence quenching.[22] A strategy to overcome this has been reported by Schmidt *et al.*, who found that cages which were conjugated to a fluorophore *via* cross-linkers could retain the desired photophysical properties of the fluorophore.[23]

3. Advantages of using metallacycles/cages over small molecular probes

Over the years, fluorescent probes based on small organic molecules have become indispensable tools for the analysis of complex cellular reactions and biologically relevant analytes. However, in many cases these probe molecules are found to be unsuitable for real-life applications. The applications of conventional fluorophores can often be limited by their propensity to undergo aggregation-caused quenching (ACQ).[24] In contrast, Tang *et al.* have developed chromophores that display aggregation-induced emission (AIE). AIE-active fluorophores (AIEgens) are nearly non-emissive as discrete molecules, but emit bright fluorescence in the aggregate state due to the restriction of their intramolecular motion.[25] Incorporation into supramolecular coordination complexes has emerged as another strategy to restrict the intramolecular rotation of AIEgens, with the resulting complexes highly fluorescent in both the solution and aggregated state. These features make AIEgens-based SCCs promising candidates for cell imaging. However, low solubility in biological milieu (under specific salt or pH conditions), non-specific interactions with biomolecules (adsorption, complexation) and poor stability (photo-/thermoresponsive degradation) can be challenging to overcome in attaining this goal.

There has been ongoing effort by scientists across the globe to use coordination-driven fluorescent supramolecular complexes for biomolecular analysis. Macrocyclic metallasupramolecules can exhibit a number of advantages over traditional organic sensors, deriving from the way in which size and geometry of the metallasupramolecules can be controlled and tailored through careful ligand design. Such advantages include:

1. Control over the size and shape of the cavities of the metallasupramolecules, enabling close-control over dimensions of the binding site for potential analytes.

2. A combination of non-covalent interactions, such as Coulombic attraction, hydrophobic effects, π-π stacking and hydrogen bonding can be engineered into the ligand design to compliment the fixed cavity size and produce hosts with high selectivity towards target analytes. Using these means the discrimination of structurally similar analytes, such as mono- and disaccharides can be attained and yield an optical response.[26]
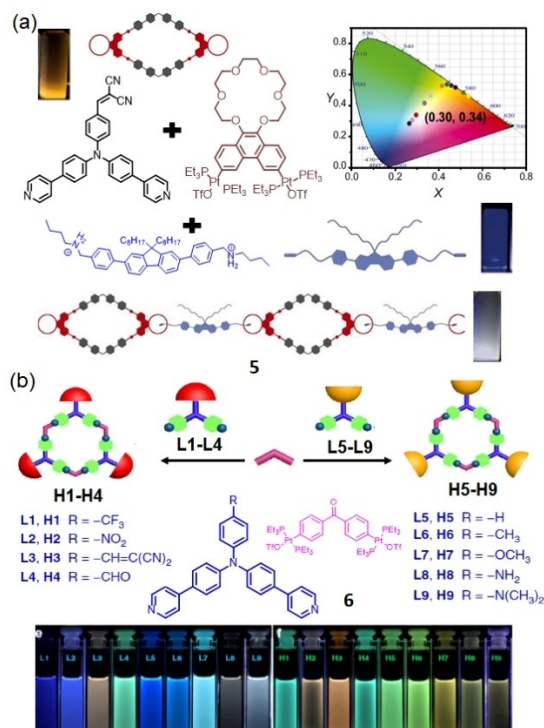

Figure 3. Effect of structural variation on the fluorescence properties of supramolecular coordination complexes, (a) **5** and (b) **6**. Reproduced from references [20] and [21] with permission from United States National Academy of Sciences and Nature Research.

ChemPlusChem

Reviews
doi.org/10.1002/cplu.202100004

Chemistry Europe
European Chemical
Societies Publishing

3. Unlike small molecule-based probes, such coordination complexes generally exhibit a 'turn-on' or ratiometric response in the presence of biomolecules, as the binding of analytes changes the conformational flexibility of metalla-cycles or their aggregation-induced emission properties. 'Turn-on' sensors are particularly suitable for biological studies since background interference is minimised.

4. The modularity of the coordination-driven self-assembly approach presents an excellent opportunity for preparing a library of metallacycle and cage systems through stepwise modification of metal and ligand building blocks.

5. Coordination-driven self-assembly enables the formation of complex architectures from relatively simple building blocks, making SCCs synthetically accessible.

4. Effect of the microenvironment on the fluorescence properties of SCCs

The intracellular environment is not homogenous, but instead contains numerous microenvironments in which properties such as viscosity, polarity, temperature, hypoxia, redox status and pH vary. These microenvironments play important biological roles in controlling molecular binding processes, enzyme activity and metabolism, intracellular transport and signal transduction.[21] For example, viscosity plays a determining role in diffusion-controlled processes and is therefore highly relevant to molecular transport and signal transduction processes. Microenvironment polarity (the hydrophilicity/hydrophobicity of localised regions) is another significant environmental factor that underpins the functions of cellular proteins and initiates signal transduction processes,[23] while the local temperature can greatly influence and control cellular functions occurring in regions including the nucleus and mitochondria.[24] Thus, it is important to verify the potential effects of different environmental factors on metallacycles/cages before their application in biomolecular sensing.

In 2019, Chakraborty et al. developed bis-terpyridine based pentameric Fe(II)-coordinated metallacycle **7** (Figure 4(a)) containing redox-active carbazole moieties.[27] When introduced into electrolyte solution, the metallacycle undergoes fast and stable colour changes from pristine purple to brown to yellow, due to the oxidation of the Fe(II) and carbazole centers in a potential window of 0–2 V. A solid-state electrochromic device fabricated with **7** (Figure 4(a)) also showed a similar multi-colour electrochromic response with rapid colouration (t_c), and bleaching times (t_b) of 2.45 and 3.49 s, respectively, along with an efficiency of 316.17 cm^2C^{-1} and cycle stability over 1000 cycles (Figure 4(b)). Similarly, Yang et al. reported the hexagonal Cu(I) metallacycle **8** containing three tris-[2] pseudorotaxane moieties (Figure 4(c)).[28] The metallacycle displayed a redox-sensitive optical response, as a change in solution colour from brown to green was observed upon oxidation. Such an optical response could plausibly be attributed to the differences in coordination geometries of $[Cu(phen)_2]^+$ and $[Cu(phen)_2]^{2+}$ in the system.
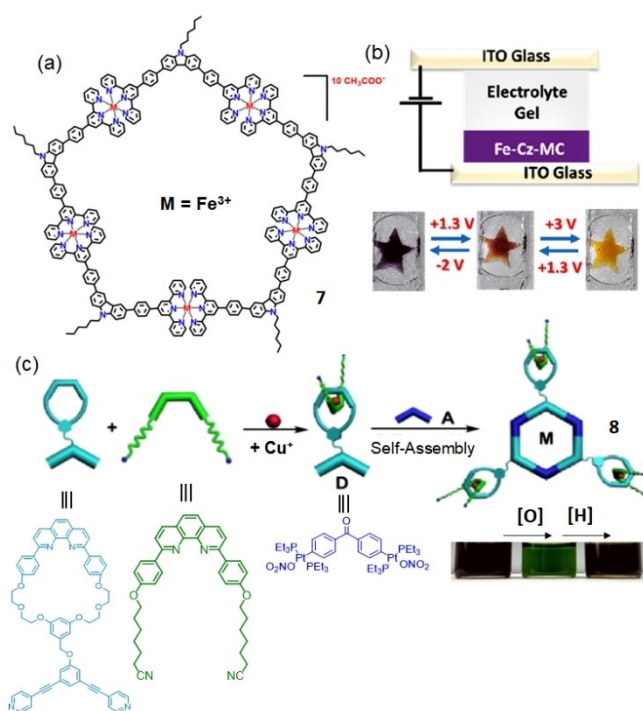

Figure 4. The structures of redox-sensitive supramolecular coordination complexes: (a) metallacycle **7**; (b) a solid-state electrochromic device incorporating **7**, and (c) metallacycle **8** and the colour changes associated with redox processes. Reproduced from references [27] and [28] with permission from the American Chemical Society.

Stang et al. have reported hexagonal metallacycles **9** and **10** via the coordination-driven self-assembly of a 120° triarylamine ligand and 120° and 180° diplatinum(II) acceptors (Figure 5(a)).[29] The metallacycles possess three and six peripherally appended anthracene groups respectively. Both metallacycles exhibited reversible changes in absorption (hypsochromic shift) and emission signals (turn-off response) in THF medium in response to varying the temperature from −20 to 60 °C. The larger metallacycle with a higher number of anthracene residues displayed a slightly higher sensitivity towards temperature change. Interestingly, in polar solvents, like DMF or CH_3CN, a ratiometric change in fluorescence colour from green to blue was observed at high temperature (70 °C), probably via a self-destruction mechanism.

The same group also reported dianthracene-based rhomboidal organoplatinum(II) metallacycle **11** which can exhibit a temperature-responsive change in fluorescence colour from cyan to yellow over a wide temperature range from 77 to 297 K in acetone medium (Figure 5(b)).[30] Similarly, Tian and co-workers have reported AIE-active tetraphenylethylene (TPE)-based Zn(II)-coordinated metallacage **12**, which showed significant increases in fluorescence intensities at a low temperature, probably due to restricted the intramolecular rotation of the TPE units (Figure 6(a)).[31] To further investigate this observation, the authors recorded the fluorescence behaviour of the cages in the solid state under variable pressure. Upon gradual increase of the external pressure, the fluorescence intensity of the metallacages enhanced initially,

ChemPlusChem

Reviews
doi.org/10.1002/cplu.202100004

**Chemistry
Europe**
European Chemical
Societies Publishing

Figure 5. (a) The structures of thermo-sensitive supramolecular coordination complexes **9**–**10**; (b) The structure and optical emission of complex **11**. Reproduced from references [29] and [30] with permission from the American Chemical Society.

Figure 6. The structures and optical responses of supramolecular coordination complexes which display (a) pressure sensitivity (**12**) and (b) pH sensitivity (**13**). Reproduced from references [31] and [32] with permission from the Chinese Chemical Society and the Royal Society of Chemistry.

due to conformational restriction of the TPE units, which was followed by quenching under 6.32 GPa, probably due to the tight packing of the supramolecules. On a similar note, Xu and co-workers designed naphthalimide-containing Pt(II)-based hexagonal metallacycle **13** which showed a turn-on yellow fluorescence response in an acetone/water (4:1, v/v) mixture when exposed to a proton source (Figure 6b).[32] The protonation of the piperazine unit could effectively inhibit photoinduced electron transfer (PET) from the piperazine to the naphthalimide moiety, leading to an enhancement in fluorescence intensity.

5. Detection of biomolecules using supramolecular coordination complexes

Molecular recognition refers to a specific interaction between host and guest molecules through either covalent bonding (chemodosimetric interaction) or non-covalent interactions. Such interactions are important for signal transduction and can produce an optical response as an output signal. Metallacycles and cages have been used for the detection of a wide-range of biomolecules, such as proteins, amino acids, carbohydrates, and biogenic amines.[12,33] While non-specific binding may occur through electrostatic interactions (relating simply to the overall charge of the complex and the analyte), careful selection of the building blocks can allow fine-tuning of the specific non-covalent interactions available within the central cavity of the host, providing a binding environment that can be tailored to the recognition of particular analytes. For example, the presence of positively charged anchoring groups such as guanidinium, pyridinium or quaternary ammonium units can provide ligand-based charge-pairing interactions regions of the host that come into closer proximity with bound guests than the metal centres.[34] Hydrogen bond donors and acceptors such as urea, thiourea, amide, acylhydrazone, phenol, imidazole, or pyrrole can initiate directional hydrogen bonding interactions with guests.[35] Analyte binding has been reported to affect the photophysical properties of the metallacycles/cages by altering the redox-status of the metal ion centres, transforming them into an electrochemical sensor.[36] Finally, in addition to non-covalent recognition pathways, biosensing can also be achieved through chemical reactions such as nucleophilic addition, substitution or hydrolysis inside the cavity of the metallacycles/cages.[37] Like small-molecule based sensors, biosensors based on supramolecular coordination complexes should also possess qualities such as high specificity, wide range of detection, low detection limit, fast response and reversibility to form an ideal indicator system.

5.1. Interaction with biogenic amines

Biogenic amines (BAs) are nitrogenous compounds, produced *via* the enzymatic decarboxylation of essential amino acids. On

ChemPlusChem

Reviews
doi.org/10.1002/cplu.202100004

**Chemistry
Europe**
European Chemical
Societies Publishing

the basis of chemical structure, BAs can be categorized in many groups, such as aliphatic diamines (e.g. cadaverine and putrescine), monoamines (e.g. 2-phenylethylamine), poly-amines (e.g. spermine and spermidine) and heterocyclic amines (e.g. histamine, tryptamine). Irrespective of their structures, almost all BAs participate in numerous metabolic processes such as growth regulation, inflammation and neural transmission. The levels of BAs in fermented food items are found to be high in general as compared to fresh food, thus elevated level of BAs can be considered as a marker of food-spoilage.[37] Considering these points, Eddaoudi and co-workers in 2019 developed a luminescent Zr(IV)-based framework **14**, encompassing a π-conjugated organic ligand with a thiadiazole functional group as the spacer (Figure 7(a)).[34] The compound exhibited a 'turn-on' fluorescence response (green fluorescence) towards aliphatic amines, including harmful nicotine with an unprecedented low detection limit (66.2 nM for methylamine) in water. Hydrogen bonding interactions between the linker unit and the guest amine molecules (in protonated form) supresses the twisting motion of thiadiazole core and significantly reduces the extent of non-radiative decay.

Stang and co-workers have employed coordination-driven self-assembled metallacycles for the vapor-phase detection of amines. The metallacycles were synthesized in-situ by mixing 1,6-di(4-pyridylvinyl) pyrene with three different aromatic dicarboxylates (**15–17**) in the presence of a 90° organo-platinum(II) complex (Figure 7(b)).[35] All of the metallacycles exhibited aggregation-induced emission (AIE) in acetone

medium, owing to π-π stacking interaction between the pyrenyl moieties of different metallacycles. When metalla-cycle-based films were exposed to different types of amine vapors, aromatic amines resulted in the quenching of yellow fluorescence, while aliphatic amines caused an increase in emission intensity with a blue-shift in λ_{max} (yellow to green fluorescence). Though no detectable structural change was observed with aromatic amines, the turn-on response by aliphatic amines was probably caused by the disassembly of the metallacycles deposited on the substrate surface. Most importantly, these kind of coordination-derived self-assembled metallacycles showed improved sensitivity towards target analytes, as demonstrated by the significantly increased response speed and decreased recovery time as compared to conventional metallacycles.

Though not a fluorometric probe, Yang *et al.* developed the rhenium metallacycle **18** as an evanescent wave infrared chemical sensor for the selective recognition of odorous amino compounds (Figure 7(c)).[36] Aliphatic and aromatic amino compounds were preferentially bound within the cavity due to a combination of supramolecular interactions, including the favourable shielding of the hydrophobic regions of the guest within the cavity of the host and interactions between the NH₂ groups in the guest and the Re(I) metal centres and the hydroxyl groups situated on the tetrahydroquinoline ligand, which are positioned at the entrance of the pocket of the Re metallacycle. The sensing response of the metallacycles was found to follow the order aromatic amine > primary amine ~ cyclo-amine > secondary amine > tertiary amine.
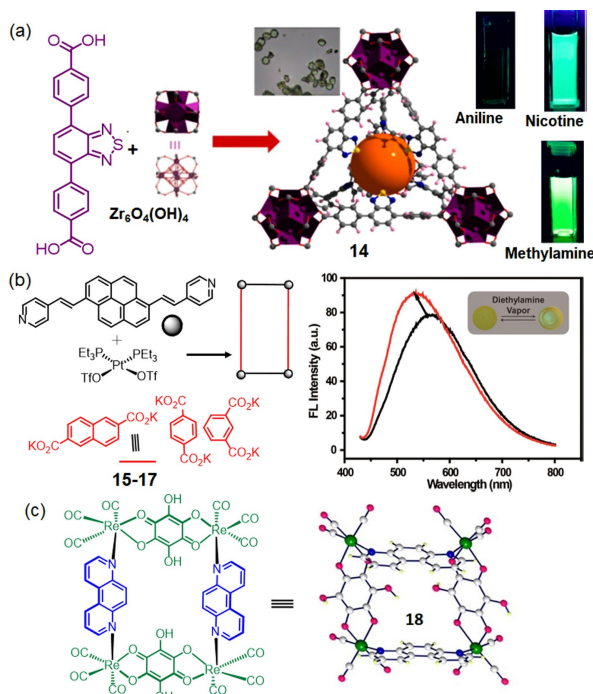

Figure 7. Structures and optical response of supramolecular coordination (a) **14**, (b) **15–17** and (c) **18** towards biogenic amines. Reproduced from references [34–36] with permission from the American Chemical Society and Elsevier.

5.2. Interaction with carboxylic acids

The design of artificial receptors for carboxylates and dicarbox-ylates is important because of the significant roles that these guests play in controlling numerous biological processes. For example, fumarate is generated as a side product in the Krebs cycle, while maleate is known as an inhibitor in the cycle.[38] In addition to small molecular probes, a number of sensory systems based on metallacycles and cages have been reported for carboxylic acids. For instance, in 2011, Chi and co-workers reported self-assembled metallacycles composed of arene-ruthenium acceptors (arene: benzoquinone, naphthacene-dione) and dipyridyl amide donors (**19** and **20**, Figure 8(a)).[39] The luminescent metallacycles so-formed showed higher bind-ing affinities and a turn-on optical response towards rigid multi-carboxylate anions such as oxalate, citrate, and tartrate compared to common monoanions such as acetate and flexible dicarboxylate anions including malonate and succinate in methanol solution. Mechanistic investigations indicated that carboxylates with complementary geometries can form hydro-gen bonds with the amidic linkage and diminish the extent of photoinduced electron-transfer from the arene-Ru moiety to the amidic donor, resulting in the turn-on fluorescence response.

Recently, Stang and co-workers have developed a series of metallacycles *via* the coordination-driven self-assembly of
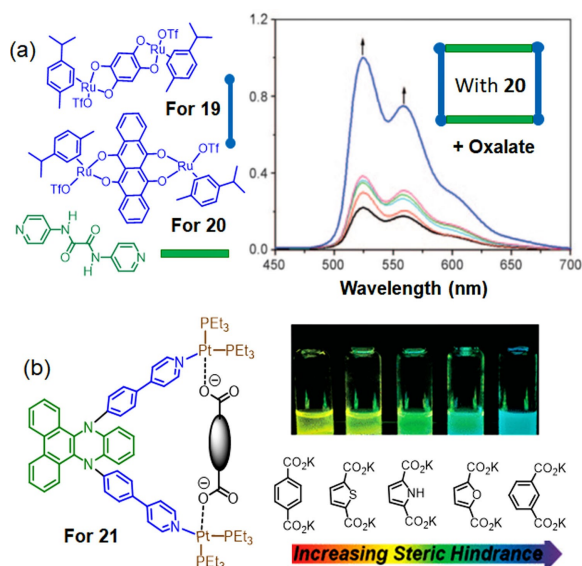
ChemPlusChem

Reviews
doi.org/10.1002/cplu.202100004

Chemistry
Europe
European Chemical
Societies Publishing

Figure 8. Structures of supramolecular coordination complexes (a) **19**–**20** and (b) **21** which have been used for optical carboxylate sensing. Reproduced from references [39] and [40] with permission from Wiley-VCH and the American Chemical Society.

Figure 9. Structures and optical responses of supramolecular coordination complexes (a) **22** and (b) **23** which have been reported as nucleotide sensors. Reproduced from references [42] and [43] with permission from the Royal Society of Chemistry and the American Chemical Society.

a phenazine-based dipyridyl ligand with various dicarboxy-lates combined with a 90° organoplatinum(II) complex (**21**) (Figure 8(b)).[40] The N,N-Disubstituted dihydrodibenzo[a,c] phenazines show excited-state planarization along the N–N axis which extends the overall π-conjugation and produces a red-shifted fluorescence signal in CH_2Cl_2 medium. Upon coordination with rigid dicarboxylates, the resultant metalla-cycles exhibited a blue-shift in λ_{max}. The extent of the blue-shift increased with decreasing bite angles (and a corre-sponding increase in steric hinderance) between the carbox-ylate building blocks, resulting in the fluorescence colour ranging from green to cyan. Interestingly, very small struc-tural differences among the dicarboxylate building blocks can be amplified into the distinct photophysical properties of the resulting metallacycles, which can be difficult to achieve in the case of small molecular probes.

5.3. Interactions with nucleotides

The development of optical probes for nucleotides has received considerable attention in recent years due to their huge biological significance. For example, adenosine triphos-phate (ATP) can not only act as universal energy source, but also actively participate in extracellular signaling processes. On the other hand, uridine triphosphate (UTP) is a key component of RNA synthesis and plays a crucial role in glycotransfer.[41] Considering the importance of these analytes, Duan and co-workers reported the Pd(II)-based truncated octahedral nano-cage **22** for the fluorescence detection of nucleosides in DMF medium in 2008 (Figure 9(a)).[42]

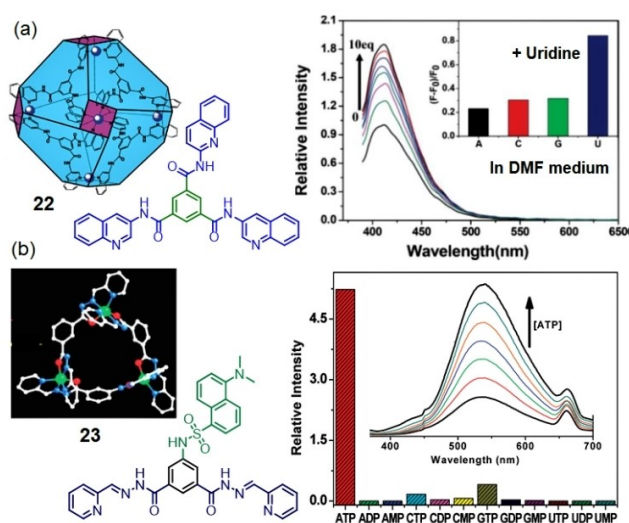The potential two-fold hydrogen bonding interactions involving amide groups make the nanocage a selective

receptor for uridine over other nucleotides. The O···N–H type hydrogen bonds are stronger than N···H–N hydrogen bonds, which explains the larger fluorescence enhancements with guanosine and uridine compared to adenosine and cytidine. Additionally, the presence of an additional acyl group in uridine probably enhances the strength of the hydrogen bonds between this nucleotide and the amide groups. Further to this work, in 2009 the same group developed a Co(II)-based helical triangle **23** consisting of dansyl fluorophore units and hydrogen bonding acylhydrazone units at meta positions of central benzene ring (Figure 9(b)).[43] The metallacycle showed a highly selective 'turn-on' response towards ATP amongst a wide range of ribonucleotide polyphosphates in a DMF-water (8: 2) mixture. Though interaction with other nucleotide triphosphates, such as GTP, CTP, or UTP were observed, the extent of fluorescence enhancement was found to be maxi-mised in the case of ATP. The ATP-specific fluorescence response might be the result of size-selective H-bonding between the nitrogenous pyrimidine base and the sulfona-mide and/or amide groups in the host, as well as electrostatic interactions between the triangular cationic backbone and the negatively charged polyphosphate unit.

As a continuation of their endeavour, in 2010 Duan *et al.* reported two different metal-organic polyhedra, octahedral nanocage **24** (containing Co-centers) and metallatricycle **25** (containing Pd-centers), comprised of fluorescent quinoline and multiple amide groups (Figure 10a).[44] The amide groups, located on the opening windows or inner surface of the polyhedra, provide ideal environments for size or shape-selective dynamic interactions with analytes. The authors suggested that two-fold hydrogen bonding interactions between the nucleosides and the amide groups in **25** made the metallatricycle selective for uridine, whereas additional H-
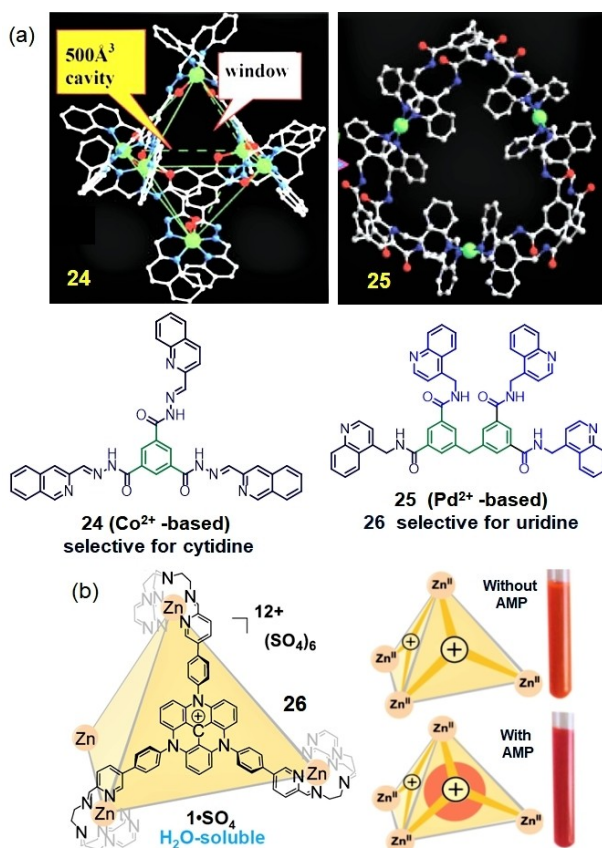
Figure 10. Structures of supramolecular coordination complexes reported for (a) nucleoside (**24**–**25**), (b) nucleoside phosphate (**26**) sensing; Reproduced from references [44] and [45] with permission from the Royal Society of Chemistry and Wiley-VCH.

in both DNA and RNA, they are still not well characterized. In RNA, 3WJs are involved in splicing and translation while in DNA, they participate in replication. Ongoing research by a number of groups has focussed on the recognition of these junctions using SCCs, and this success could pave the way for optical detection strategies in the future.

In 2006 Hannon *et al.* designed a tetracationic metallosupramolecular helicate **27**, composed of three bis-pyridylimine organic strands wrapped about two Fe^{2+} ions. This metal-helicate could selectively recognized 3WJs (Figure 11(a)).[46] Structural analysis indicated that the probe could occupy the central hollow space of the 3WJ, where the axially located two Fe^{2+} ions would enhance the stability of the complex by electrostatic interactions. In addition, the metal-helicates also possess a large hydrophobic surface owing to the presence of 12 aromatic rings, and could this participate in π-stacking interactions with thymine and adenine bases (Figure 11(b)). Further work from Hannon identified that the precise size, shape and chirality of the cylinder plays a key role in stabilization of DNA structure[47] with the M helical isomer forming a more stable complex due to the P isomer causing inversion of the helical sense of the twist at the junction (a destabilising effect). Meanwhile, Sletten *et al.* have performed detailed ^{1}H-NMR studies to elucidate interaction of this type of tetracationic supramolecular helicate with 3WJs,[48] confirming that that the helicate can fit into the center of the 3WJ.

Scott and co-workers have also studied the interaction of the diastereomerically pure, flexible helicate **28** with short
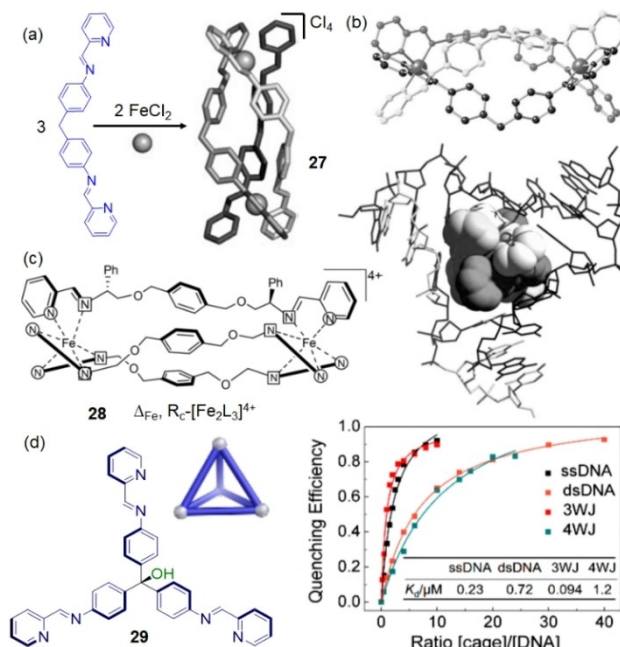
bonding involving active CH-moieties was responsible for a cytidine-specific response in the case of **24**.

In 2019 Nitschke and co-workers reported the tetrahedral Zn(II)-coordination cage **26** formed from subcomponents based on cationic triazatriangulenium (TATA$^+$) groups, as shown in Figure 10(b).[45] The integration of the fluorescent TATA$^+$ units into the ligand scaffold increased the overall positive change of the tetrahedron from 8+ to 12+, while the extended aromatic structure created a large cavity suitable for guest recognition. The metallacages showed preferential binding with negatively charged biomolecules over positively-charged or neutral ones, and thus differentiable responses were observed between adenosine *vs* adenosine monophosphate and guanosine *vs* guanosine monophosphate. However, no significant alteration in binding strength was observed upon increasing the magnitude of the negative charge of the guest. It can be envisioned that the polyanionic backbone of the more highly charged nucleotides improves their interaction with water, counterbalancing any greater electrostatic attraction to the metallacages.

DNA junctions are unique branched structures where several double strands converge at one point. The three-way junction (3WJ) is the simplest and one of the most abundant branched nucleic acid structures. Though 3WJs can be found

Figure 11. (a) The structure of supramolecular metal-helicate **27** reported for recognition of 3-way junction DNA structure (3WJ). (b) X-ray single crystal structure of **27** and its interaction with 3WJ; (c) The diastereomerically pure metal-helicate **28** for detection of 3WJ. (d) The structure of cage **29** which has been reported to bind to fluorescently labelled DNA, yielding an optical response. Reproduced from references [46,49,50] with permission from Wiley-VCH, Oxford University Press and the American Chemical Society.

ChemPlusChem

Reviews
doi.org/10.1002/cplu.202100004

Chemistry
Europe
European Chemical
Societies Publishing

duplex DNA sequences containing abasic (AP) sites (Figure 11(c)).[49] They found that the so-called "flexicates" could bind to AP sites in a shape-selective manner, particularly to AP sites flanked by purines on both sides. The binding affinity was further enhanced when a pyrimidine was placed in opposite orientation to the lesion. By using DNA structures containing 2-aminopurine (2AP, a fluorescent analogue of adenine) the authors observed a fluorescence response to flexicate binding, with the binding of the flexicate causing fluorescence quenching. A further optical readout upon flexicate binding was established based on the displacement of amiloride, a fluorescent molecule known to recognise thymine situated opposite an AP site. In 2019 Keyser, Nitschke and co-workers reported that a water-soluble $Fe^{II}_4L_4$ tetrahedron **29** could bind to single stranded DNA, mismatched DNA base pairs, and three-way DNA junctions in aqueous buffer solutions (Figure 11(d)).[50] The binding of the cages could be observed through the quenching of a proximate fluorophore, thus providing an optical readout to monitor the interaction and assess the distance of the binding site from the fluorescent label present on the DNA backbone. The preferential binding with ss-DNA ($I/I_0 \sim 69\%$) and three-way junction DNA ($I/I_0 \sim 75\%$) over ds-DNA and 4WJ (four-way DNA junction) was hypothesised to relate to the trigonal three-dimensional shape of the tetrahedral cage. As it was observed that DNA-cage binding occurred specifically at unpaired bases, the authors further explored the potential of the metallacages to sense base-pair mismatches in dsDNA.
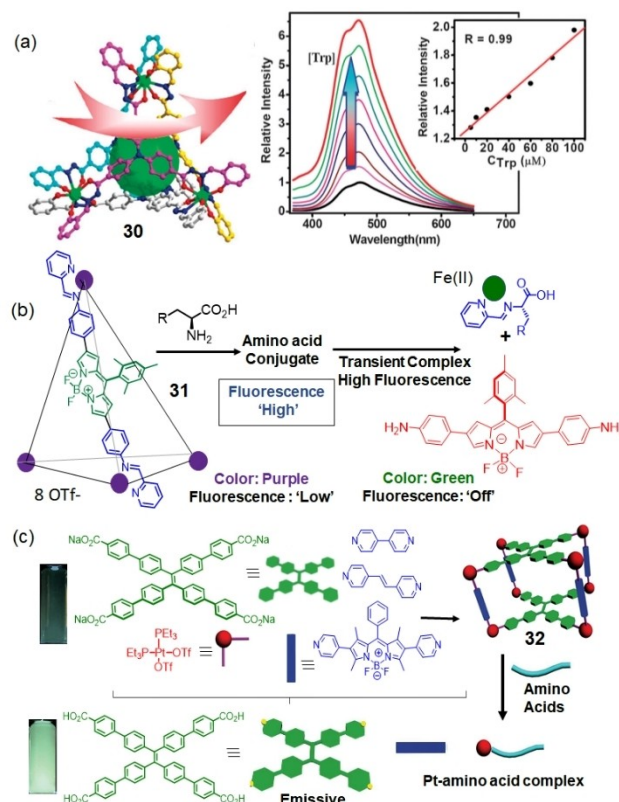

Figure 12. Structures and optical responses of supramolecular coordination complexes (a) **30**, (b) **31** and (c) **32** which have been reported for amino acid sensing. Reproduced from references [51–53] with permission from the Royal Society of Chemistry.

5.4. Interactions with amino acids

Recently, increasing attention towards the treatment, prevention and early-diagnosis of diseases has directed the development of new methods for the detection of essential amino acids. Depending upon the functional group of the side chain, amino acids play an active role in maintaining various physiological processes. For example, lysine (Lys) is closely related to the Krebs-Henseleit cycle and plays a pivotal role in polyamine synthesis, whereas histidine (His) is indispensable for the growth and repair of tissues.[54] Considering such multifaceted roles in biological systems, in 2012 Duan et al. reported the design and synthesis of cerium-based tetrahedron **30** comprising twelve hydrogen-bonding amide linkages and four triphenylamine units as luminophores with potential π-stacking ability (Figure 12(a)).[51] The cage showed a selective turn-on fluorescence response towards tryptophan and tryptophan-containing peptides in DMF-water mixtures through the combined effects of hydrogen bonding, π-stacking and size/shape matching. Considering the high sensitivity as well as selectivity, this cage was also employed for the in-vitro quantification of tryptophan in human blood serum samples.

In 2014 Nitschke and co-workers reported a series of purple fluorescent coordination cages **31** (Figure 12(b)) by incorporating BODIPY and pyrene fluorophores.[52] These M_4L_6 tetrahedral cages were then employed for the detection of amino-acids with a turn-on response in a 50% acetonitrile-water mixture. However, upon standing for ~5 hours, the absorption maximum of the mixture (M_4L_6 + amino acids) was red-shifted, accompanied by the complete disappearance of fluorescence intensity. It was concluded from experimental evidence that initially the amino acids formed highly fluorescent coordination complexes with the cages; however, these transiently formed complexes were unstable, and substitution of the BODIPY-based imines with amino acid centred imines triggered the release of a free bis(aminophenyl)BODIPY component (green fluorescence). Similarly, in 2017 Stang and co-workers developed a series of tetragonal prismatic Pt(II) metallacages (**32**, Figure 12(c)). The cages contained benzoate-TPE groups to define two faces, dipyridyl ligands to construct four pillars, and 90° Pt(II) acceptors as the eight corners.[53] The metal-coordination partially restricts the intramolecular rotations of the TPE units, which makes the cages emissive even in dilute conditions. On the other hand, fluorescence maxima were tuned by variation of the dipyridyl ligands. The addition of H_2S and thiol-containing amino acids resulted in a turn-on fluorescence response in a methanol-water (1:1) mixture medium (in which the cage alone was nearly non-emissive) though a self-destructive mechanism and the competitive formation of Pt(II)-amino acid complexes.

ChemPlusChem

Reviews
doi.org/10.1002/cplu.202100004

**Chemistry
Europe**
European Chemical
Societies Publishing

5.5. Interactions with proteins

Proteins are large biopolymers composed of hundreds of amino acid residues, with pivotal roles in biological processes including catalysing metabolic reactions, DNA replication and mediating cellular transport processes. The primary structures of proteins depend on the sequence of amino acids, which is dictated by the nucleotide sequence of their genes. These primary structures eventually control the 3D-protein folding and determine their functions.[49] In 2014, Chi and co-workers reported the new [2+2] wedge-like metallacycles (**33**, Figure 13(a)), where N, N'-bis(4-(pyridin-4-ylethynyl)phenyl) pyridine-2,6-dicarboxamide ligands are connected through diruthenium arene complexes.[55] The metallacycle binds to the enhanced green fluorescent protein (EGFP) variant of GFP, resulting in quenching of the blue-fluorescence usually emitted by the protein. Mechanistic studies indicated that the metallacycles interact with EGFP through the Arg168 residue and induce a conformational change by disrupting the tripeptide chromophore. Such binding eventually led to the aggregation of the EGFP protein, as evidenced by gel electrophoresis, circular dichroism and atomic force microscopy studies. In 2015, Furrer *et al.* studied the interactions of three different hexacationic arene ruthenium metallaprisms (**34–36**, Figure 13(b)) with a series of human proteins.[56] Among the different proteins studied, human serum albumin and transferrin lead to precipitation, while three cytosolic proteins - cytochrome c, myoglobin and ubiquitin – induced changes in the CD (circular dichroism) signal ascribed to structural alterations to the protein.

In 2017 Stang *et al.* reported the tetraphenylethylene (TPE)-based organoplatinum(II) metallacycle **37**, which could bind to the negatively charged surface of the rod-like tobacco

mosaic virus (TMV) and form 3D-micrometer-sized bundle-like superstructures in an aqueous medium (Figure 13(c)).[57] Due to the nano-confinement effect and the aggregation-induced emission (AIE) of the TPE units, the resultant metallacycle-protein composite showed a dramatic fluorescence enhancement compared to the parent metallacycle. Disruption of these metal-organic biohybrid materials and subsequent release of **37** was observed in the presence of tetrabutylammonium bromide (TBAB). TBAB is a surfactant which disassembles the TMV/TPE—Pt—MC composite. In order to prove the generality of this approach, the authors subsequently examined whether other negatively charged protein-based species such as bacteriophage M13 and ferritin could form fluorescent nano-bio composites with **37**.

5.6. Interactions with carbohydrates

Following seminal work by Czarnik and Yoon in 1992, a large number of small molecular probes have been reported in recent years for the fluorescence sensing of saccharides.[58] Most of these probes involve boronic acids as the primary receptor component due to their ability to form boronate esters specifically in presence of cis-diols. In spite of excellent sensitivity, most of these probes show preferential interactions with D-fructose (or sometimes with D-glucose). Thus, there is strong research interest in developing sensory systems for other carbohydrate molecules, including both disaccharides and polysaccharides.[59] Considering these issues, in 2008 Yan and co-workers developed a novel strategy for preparing metal-tunable octahedral nanocages for potential biosensing applications.[60] Quinoline groups were used as a signalling unit and also help to define the proper size for guest-encapsulation, while hydrazone residues were chosen to participate in H-bonding interactions with guest molecules. The Zn(II)-based metallacycle **38** showed fluorescence enhancement on the addition of glucosamine in acetonitrile medium (Figure 14(a)). Mechanistic investigations indicated that glucosamine formed an inclusion complex with the positively-charged cages, which were stabilized by H-bonding interactions between multiple amide groups and the saccharide.

In 2009, Duan *et al.* reported the Ce-based Werner type tetrahedra (**39** and **40**, Figure 14(b)) for size-specific luminescent sensing of neutral carbohydrates in a DMF-acetone (5:95 v/v) solution.[26a] The probe **39** with a smaller cavity-size (inner volume: 300 Å^3) showed larger luminescence emission intensity in the presence of hexoses, such as mannose or glucose in comparison to pentose sugars. Similarly, cage **40** with a larger cavity (inner volume: 550 Å^3) showed a higher binding affinity towards disaccharides over the smaller-sized monosaccharides.

In a similar approach, the same group also reported the size-specific selective recognition of neutral carbohydrates using two M_4L_4 molecular tetrahedra (**41** and **42**, Figure 14(c)) by incorporating amide groups into the building blocks.[26b] The smaller tetrahedron **41** showed fluorescence enhancement specifically upon addition of natural monosac-
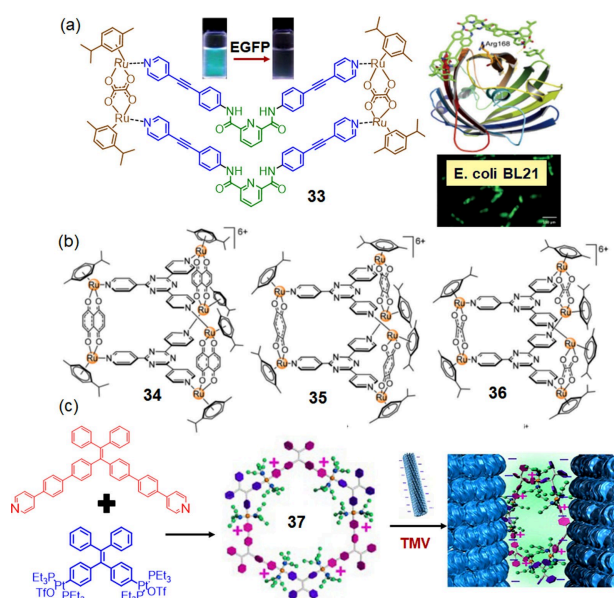

Figure 13. Structures of supramolecular coordination complexes (a) **33**, (b) **34–36** and (c) **37** reported for protein sensing. Reproduced from references [55–57] with permission from the Royal Society of Chemistry and the American Chemical Society.
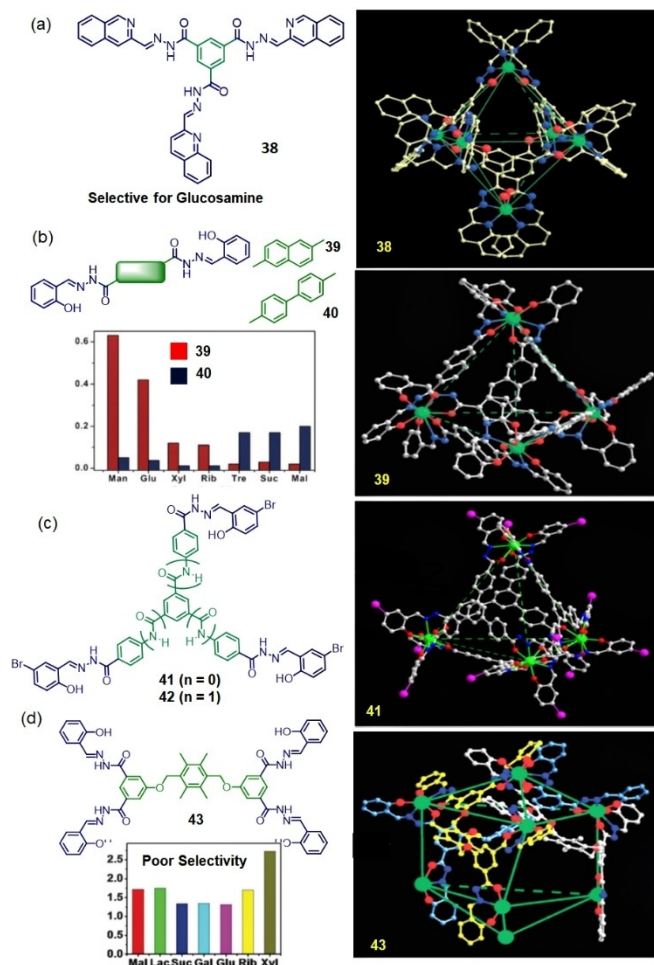
ChemPlusChem

Reviews
doi.org/10.1002/cplu.202100004

Chemistry Europe
European Chemical
Societies Publishing

Figure 14. Structures of supramolecular coordination complexes (a) **38**, (b) **39**–**40**, (c) **41**–**42**, (d) **43** reported for carbohydrate sensing. Reproduced from references [60] and [26a–c] with permission from Wiley-VCH, the Royal Society of Chemistry and Elsevier.

based triangular prism **44** and tetranuclear tetrahedron **45** containing 36 and 24 amides within their backbones respectively (Figure 15(a)).[26d] Among a wide-range of carbohydrates, **44** showed excellent selectivity towards lactose, while **45** exhibited preferential interactions with sucrose. It was proposed that changing the topology of the cages along with the spatial arrangement of hydrogen binding sites in the confined space of the host could modify the selectivity towards guest molecules.

In 2017 Yamashina and co-workers developed the Pt(II)-coordination-driven molecular capsule **46** surrounded by polyaromatic anthracene panels, with a spherical cavity of ~1 nm diameter and ~580 Å^3 volume (Figure 15(b)).[26e] The nanocapsule could effectively encapsulate D-sucrose from a mixture of different natural disaccharides in water (~100% selectivity, >85% yield, and $K_a \geq 1100$ M^{-1}). Unlike the previous examples, where interactions with saccharides are primarily controlled by H-bonding interactions, here the unique selectivity is mainly attributed to multiple CH-π interactions between sucrose and the polyaromatic cavity.

Recently Yang and co-workers synthesized a hexagonal organoplatinum(II) metallacycle **47** for the selective detection of heparin, a sulfated glycosaminoglycan polymer (Figure 16(a)).[61] The electrostatic interaction between the positively charged metallacycle and the negatively charged heparin resulted in the formation of higher-order aggregates with typical AIE behavior (originating from the restricted motion of the TPE moieties). Thus, a ~10-fold increase in fluorescence intensity was witnessed selectively upon addition of heparin in aqueous media.
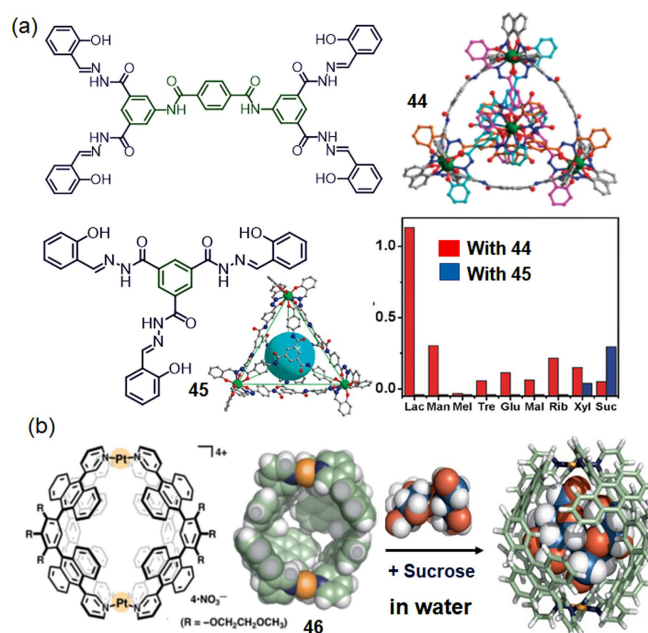
charides, whereas the larger analogue **42** with twelve additional free amide groups exhibited excellent selectivity towards sucrose over other mono- and di-saccharides. The highly specific response towards sucrose was attributed to both the dimensions of the cavity as well as the hydrogen bond interactions with the amide groups. The importance of balancing these factors was highlighted by work from the same authors in 2011. Duan *et al.* developed the Ce-based bicoronal trigonal prism **43** incorporating NOO tridentate metal chelators units for a similar purpose (Figure 14(d)).[26c] The inner volume of **43** was estimated as 750 Å^3 with 8.0 Å opening edges. Though luminescence enhancement was observed with a large number of monosaccharides or disaccharides, no size-specific selectivity pattern could be traced. The low selectivity toward these saccharides indicates that the cage was large enough to fully encapsulate the oligosaccharides studied regardless of their size, but lacked the preorganized inward-directed H-bonding sites essential for specific interactions. This short-coming was quickly addressed when the same group designed the octa-nuclear bicoronal Ce-

Figure 15. Structures of supramolecular coordination complexes (a) **44**–**45** (b) **46** reported as carbohydrate sensors. Reproduced from references [26d,e] with permission from the Royal Society of Chemistry and the American Association for the Advancement of Science.
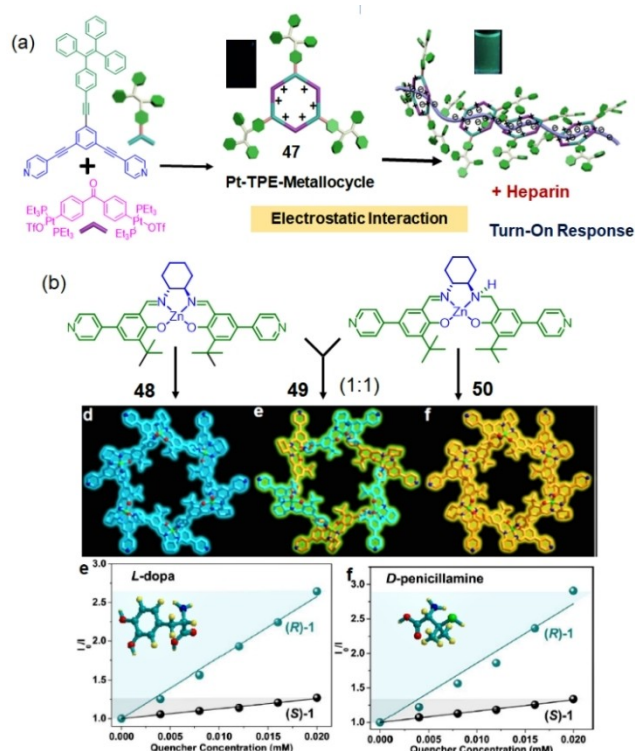
ChemPlusChem

Reviews
doi.org/10.1002/cplu.202100004

Chemistry Europe
European Chemical
Societies Publishing

Figure 16. Structures of supramolecular coordination complexes for (a) heparin sensing (**47**) and (b) the detection of chiral biomolecules (**48–50**). The optical response to binding the (*R*)- and (*S*)-enantiomers of dopamine and penicillamine are shown. Reproduced from references [61] and [63] with permission from the American Chemical Society.

5.7. Interactions with chiral biomolecules

Chirality is a prominent feature of the building blocks of life, with biomolecules including amino acids, proteins, sugars and nucleic acids existing in only one of two possible enantiomers in natural systems. Most importantly, chirality can influence the functional properties of biomolecules. For example, dextrorotatory sugars can easily be metabolized by enzymes present in the human body, while left-handed sugars show resistance towards such changes. Similarly, two enantiomers of a molecule may contribute to different tastes and smells. For instance, the two different enantiomeric (+) and (−) forms of limonene present in oranges and lemons are responsible for the differences in smell.[62] Thus, enantioselective recognition and sensing is an important research goal.

Cui *et al.* have reported the preparation of chiral NH-controlled supramolecular Zn₆(salen)₆ metallacycles **48–50** via the assembly of enantiopure pyridyl-functionalized metal-lasalalens and/or metallasalens (Figure 16(b)).[63] The metallacycles showed enantioselective fluorescence quenching with α-hydroxycarboxylic acids, amines, amino acids and a few selected small pharmaceutical molecules such as L-DOPA and D-Penicillamine. Additionally, the metallacycles could discriminate between the enantiomers of 1-phenylethylamine *via* a turn-on fluorescence response in the crystalline state. The selectivity and the binding affinity were influenced by the

number and spatial distribution of the NH groups in the chiral metallacycles. The authors attributed the observed chiral discrimination to the chiral micro-environment of the metallacycles, with the change in fluorescence emission caused by a donor-acceptor electron-transfer process upon guest uptake.

Similarly, Mirkin and co-workers developed Pt(II)-based calix[4]arene linked metallacycles via the Weak-Link Approach.[64] They noticed that controlling the coordination environment of the Pt(II) centers could transform the resulting metallacycle from a rigid, cationic configuration to a flexible, neutral architecture, which modified the binding selectivity and sensitivity towards target analytes. The cationic metallacycle **51**, having a large internal cavity defined by flexible ligands containing uncoordinated thioether linkages showed preferential binding with dextromethorphan-HCl (Figure 17(a)). It was further speculated that cationic substrates, such as those containing ammonium groups, may be further stabilised through cation-π interactions with the electron-rich cavitands. In contrast, the neutral receptor **52** possessed a smaller and more rigid cavity with a greater local electrostatic charge (Figure 17(b)). Thus, rather than binding cationic guests it was found to encapsulate neutral hydrophobic guests such as estradiol *via* favorable C–H/π interactions.

5.8. Interactions with volatile organic molecules

Recently, the environmental impact of volatile organic compounds (VOCs) have come under scrutiny due to their large-scale production as well as their use in manufacturing industries.[66] Additionally, long-term exposure to VOCs causes a wide range of health problems, including eyes, nose and throat irritation, nausea, and damage to the kidneys, liver and nervous system. For example, the uncontrolled secretion of nitric oxide (NO) in the human body triggers the production of
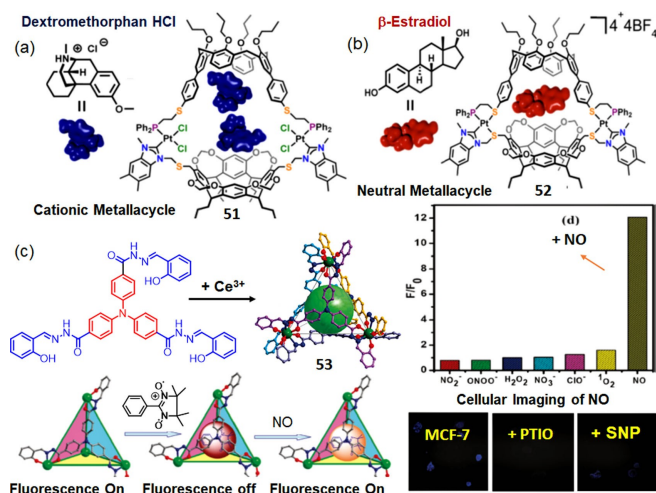

Figure 17. Structures of supramolecular coordination complexes involved in (a-b) chiral biomolecule (**51–52**); (c) The structure of cage **53** which has been reported for nitric oxide sensing in solution and in cells. Reproduced from references [64] and [65] with permission from the American Chemical Society.

ChemPlusChem

Reviews
doi.org/10.1002/cplu.202100004

Chemistry
Europe
European Chemical
Societies Publishing

reactive oxygen species, which further causes several health problems, including endothelial dysfunction, neurodegeneration and inflammation.

In 2011 Duan *et al.* synthesized a Ce$_4$(H$_2$TTS)$_4$ tetrahedron **53** that could be employed for fluorescence imaging of NO in living cells (Figure 17(c)).[65] The tetrahedral cage encapsulated the spin-trapping agent molecule nitronyl nitroxide, which led to quenching of the blue fluorescence that originated from the triphenylamine moiety in the ligand. In the presence of NO the encapsulated nitronyl nitroxide underwent a spin trapping reaction with NO within the cavity and regenerated the native fluorescence of the triphenylamine residues. The authors also performed the imaging of intracellular NO in MCF-7 cells using this probe.

Yang and co-workers designed the fluorescent metallacycle **54** that contained a peripheral alkynylplatinum(II) bzimpy group (Figure 18(a)).[67] The metallacycle showed a visible colour change from yellow to red upon exposure to CH$_2$Cl$_2$ vapour, (classified as a probable carcinogen). Interestingly, unlike other vapochromic materials, this metallacycle could retain its red colour in air over a period of months at room temperature or under vacuum for over one week. Mechanistic studies indicated that after exposure to CH$_2$Cl$_2$ vapour, the metallacyclic scaffold adopted a chair conformation which favoured a closely stacked structure due to intermolecular Pt···Pt and π-π stacking interactions. The resulting close-packed structure was highly stable, even upon the removal of the CH$_2$Cl$_2$ molecules. The red metallacycle material could be reverted to the original yellow powder by mechanical grinding. Similarly, Stang and co-workers developed rectangular organoplatinum(II) metallacycles **55** and **56** formed via coordination-driven self-assembly of 9,10-di(4-pyridylvinyl)anthracene (DPA) with different dicarboxylate

ligands in the presence of a 90° organoplatinum(II) acceptor (Figure 18(b)).[68]

Due to the presence of an AIE-active ligand, 9,10-di(4-pyridylvinyl)anthracene, both of these metallacycles showed both AIE (near-infrared fluorescence in the solid state) and solvatochromism. Both of the metallacycles showed a red to yellow colour change when exposed to ammonia vapor. The authors proposed that the Pt–N coordination bonds in the metallocycles were cleaved in the presence of ammonia, leading to a change in colour and fluorescence signal. Interestingly, this bond cleavage was reversible and the removal of the ammonia vapor regenerated the original red colour through reforming the broken coordinate bonds.

6. Concluding remarks and future directions

Supramolecular coordination complexes have emerged as effective host materials for a wide range of biologically relevant analytes. Unlike small molecular probes, in many cases binding to biomolecules leads to either a turn-on or ratiometric fluorescence response. It is worthy of note that 'turn-on' probes are more effective than 'turn-off' sensors due to high signal to noise ratios, which results in reduced background interference. However, ratiometric probes are superior to both 'turn-on' or '-off' sensors as they consider changes in optical signal simultaneously at two different wavelengths, thus nullifying any interference from the surrounding environment. The host-guest interactions in SCCs are mostly dominated by the size and shape of the cavity, the presence of functional groups on the spacer as well as the nature of the metal ions (hydration, coordination number, electrophilicity). Additionally, the mode of interaction with SCCs depends on the nature of the target analytes. For example, small hydrophobic guests with proper shape/ size can fit into the hydrophobic cavity of the SCCs, whereas negatively charged molecules can initiate charge-pairing interactions with metal ion centers. Similarly, analytes having multiple -NH or -OH units, such as carbohydrates or proteins can be engaged in hydrogen-bonding interactions with hydrophilic spacer units. These kinds of multipoint interactions with target analytes can be used to infer binding selectivity, even amongst structurally similar guest molecules. Interestingly, the encapsulation of guest molecules can lead to rigidification of host metallacycles/cages, resulting in a decrease in the extent of non-radiative decay.

Despite these advantages, the use of SCCs in biomolecular analysis remains somewhat restricted, and challenges remain before such systems can reach their full potential as components of biosensory devices. These include (a) the solubility and potential aggregation of SCCs in biological media (buffered medium, serum-rich conditions, high ionic-strength); (b) high susceptibility towards surrounding environment (influenced by pH, temperature, viscosity); (c) potential decomposition pathways which can be triggered by factors such as pH, competitive chelation of biologically abundant metal ions (such as Fe, Cu, and Zn) and amino acids (such as
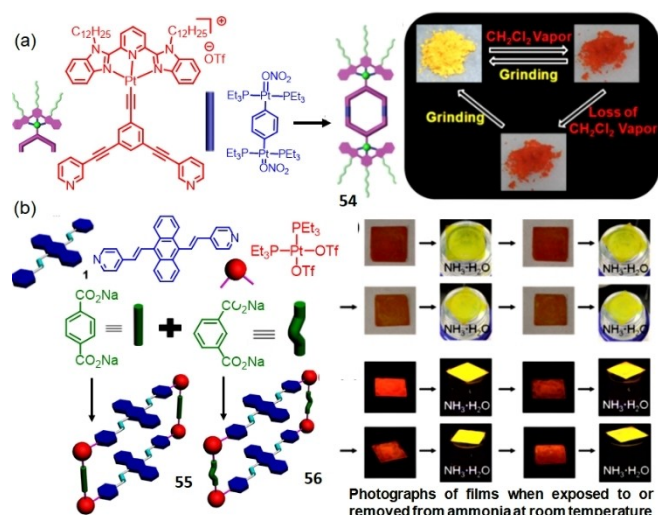
Figure 18. Structures of supramolecular coordination complexes (a) **54** and (b) **55–56** reported for the detection of volatile organic molecules. The solid-state optical response of the structure to guest binding is illustrated. Reproduced from references [67] and [68] with permission from the American Chemical Society.

cysteine, tryptophan, tyrosine, glutamic acid, aspartic acid). These factors remain as key challenges to address for further applications of this technology.

Conflict of Interest

The authors declare no conflict of interest.

[1] a) T. R. Cook, Y.-R. Zheng, P. J. Stang, *Chem. Rev.* **2013**, *113*, 734–777; b) A. Casini, B. Woods, M. Wenzel, *Inorg. Chem.* **2017**, *56*, 14715–14729; c) L. Xu, Y.-X. Wang, H.-B. Yang, *Dalton Trans.* **2015**, *44*, 867–890; d) A. Pöthig, A. Casini, *Theranostics* **2019**, *9*, 3150–3169; e) Y.-L. Lai, X.-Z. Wang, R.-R. Dai, Y.-L. Huang, X.-C. Zhou, X.-P. Zhou, D. Li, *Dalton Trans.* **2020**, *49*, 7304–7308; f) B. Li, T. He, Y. Fan, X. Yuan, H. Qiu, S. Yin, *Chem. Commun.* **2019**, *55*, 8036–8059; g) Y.-X. Hu, X. Zhang, L. Xu, H.-B. Yang, *Isr. J. Chem.* **2019**, *59*, 184–196.
[2] H. Sepehrpour, W. Fu, Y. Sun, P. J. Stang, *J. Am. Chem. Soc.* **2019**, *141*, 14005–14020.
[3] X. Hu, J. Chai, C. Zhang, J. Lang, S. P. Kelley, S. Feng, B. Liu, D. A. Atwood, J. L. Atwood, *J. Am. Chem. Soc.* **2019**, *141*, 9151–9154.
[4] X. Ma, R. Sun, J. Cheng, J. Liu, F. Gou, H. Xiang, X. Zhou, *J. Chem. Educ.* **2016**, *93*, 345–350.
[5] K. Acharyya, S. Bhattacharyya, H. Sepehrpour, S. Chakraborty, S. Lu, B. Shi, X. Li, P. S. Mukherjee, P. J. Stang, *J. Am. Chem. Soc.* **2019**, *141*, 14565–14569.
[6] J. Li, J. Wang, H. Li, N. Song, D. Wang, B. Z. Tang, *Chem. Soc. Rev.* **2020**, *49*, 1144–1172.
[7] I. V. Grishagin, J. B. Pollock, S. Kushal, T. R. Cook, P. J. Stang, B. Z. Olenyuk, *Proc. Natl. Acad. Sci. USA* **2014**, *111*, 18448–18453.
[8] a) C. J. E. Haynes, J. Zhu, C. Chimerel, S. Hernández-Ainsa, I. A. Riddell, T. K. Ronson, U. F. Keyser, J. R. Nitschke, *Angew. Chem. Int. Ed.* **2017**, *56*, 15388–15392; *Angew. Chem.* **2017**, *129*, 15590–15594; b) M. Jung, H. Kim, K. Baek, K. Kim, *Angew. Chem. Int. Ed.* **2008**, *47*, 5755–5757; *Angew. Chem.* **2008**, *120*, 5839–5841; c) R. Kawano, N. Horike, Y. Hijikata, M. Kondo, A. Carné-Sánchez, P. Larpent, S. Ikemura, T. Osaki, K. Kamiya, S. Kitagawa, S. Takeuchi, S. Furukawa, *Chem* **2017**, *2*, 393–403.
[9] a) L. He, L.-X. Cai, M.-H. Li, G.-L. Zhang, L.-P. Zhou, T. Chen, M.-J. Lin, Q.-F. Sun, *Chem. Sci.* **2020**, *11*, 7940–7949; b) G. I. Dzhardimalieva, L. N. Rabinskiy, K. A. Kydralieva, I. E. Uflyand, *RSC Adv.* **2019**, *9*, 37009–37051.
[10] B. Woods, R. D. M. Silva, C. Schmidt, D. Wragg, M. Cavaco, V. Neves, V. F. C. Ferreira, L. Gano, T. S. Morais, F. Mendes, J. D. G. Correia, A. Casini, *Bioconjugate Chem.* **2021**, DOI: 10.1021/acs.bioconjchem.0c00659.
[11] P. H. Dinolfo, J. T. Hupp, *Chem. Mater.* **2001**, *13*, 3113–3125.
[12] N. Ahmad, H. A. Younus, A. H. Chughtai, F. Verpoort, *Chem. Soc. Rev.* **2015**, *44*, 9–25.
[13] Y. Sun, C. Chen, J. Liu, L. Liu, W. Tuo, H. Zhu, S. Lu, X. Li, P. J. Stang, *J. Am. Chem. Soc.* **2020**, *142*, 17903–17907.
[14] J. E. M. Lewis, E. L. Gavey, S. A. Cameron, J. D. Crowley, *Chem. Sci.* **2012**, *3*, 778–784.
[15] a) B. Woods, M. N. Wenzel, T. Williams, S. R. Thomas, R. L. Jenkins, A. Casini, *Front. Chem.* **2019**, *7*; b) J. Han, A. Schmidt, T. Zhang, H. Permentier, G. M. M. Groothuis, R. Bischoff, F. E. Kühn, P. Horvatovich, A. Casini, *Chem. Commun.* **2017**, *53*, 1405–1408.
[16] Y. Zhang, S. Yuan, G. Day, X. Wang, X. Yang, H.-C. Zhou, *Coord. Chem. Rev.* **2018**, *354*, 28–45.
[17] T. R. Cook, V. Vajpayee, M. H. Lee, P. J. Stang, K.-W. Chi, *Acc. Chem. Res.* **2013**, *46*, 2464–2474.
[18] Z. Zhou, X. Yan, M. L. Saha, M. Zhang, M. Wang, X. Li, P. J. Stang, *J. Am. Chem. Soc.* **2016**, *138*, 13131–13134.
[19] X. Yan, M. Wang, T. R. Cook, M. Zhang, M. L. Saha, Z. Zhou, X. Li, F. Huang, P. J. Stang, *J. Am. Chem. Soc.* **2016**, *138*, 4580–4588.
[20] M. Zhang, S. Yin, J. Zhang, Z. Zhou, M. L. Saha, C. Lu, P. J. Stang, *Proc. Natl. Acad. Sci. USA* **2017**, *114*, 3044–3049.
[21] J.-L. Zhu, L. Xu, Y.-Y. Ren, Y. Zhang, X. Liu, G.-Q. Yin, B. Sun, X. Cao, Z. Chen, X.-L. Zhao, H. Tan, J. Chen, X. Li, H.-B. Yang, *Nat. Commun.* **2019**, *10*, 4285.
[22] A. Schmidt, M. Hollering, M. Drees, A. Casini, F. E. Kühn, *Dalton Trans.* **2016**, *45*, 8556–8565.
[23] a) A. Schmidt, M. Hollering, J. Han, A. Casini, F. E. Kühn, *Dalton Trans.* **2016**, *45*, 12297–12300; b) B. Woods, D. Döllerer, B. Aikman, M. N. Wenzel, E. J. Sayers, F. E. Kühn, A. T. Jones, A. Casini, *J. Inorg. Biochem.* **2019**, *199*, 110781.
[24] H.-X. Yu, J. Zhi, Z.-F. Chang, T. Shen, W.-L. Ding, X. Zhang, J.-L. Wang, *Mat. Chem. Front.* **2019**, *3*, 151–160.
[25] M. Gao, B. Z. Tang, *ACS Sens.* **2017**, *2*, 1382–1399.
[26] a) Y. Liu, X. Wu, C. He, Y. Jiao, C. Duan, *Chem. Commun.* **2009**, 7554–7556; b) J. Zhang, C. He, C. Duan, *Inorg. Chem. Commun.* **2014**, *49*, 140–142; c) L. Zhao, S. Qu, C. He, R. Zhang, C. Duan, *Chem. Commun.* **2011**, *47*, 9387–9389; d) Y. Jiao, J. Zhang, L. Zhang, Z. Lin, C. He, C. Duan, *Chem. Commun.* **2012**, *48*, 6022–6024; e) M. Yamashina, M. Akita, T. Hasegawa, S. Hayashi, M. Yoshizawa, *Sci. Adv.* **2017**, *3*, e1701126-e1701126.
[27] S. Roy, C. Chakraborty, *ACS Appl. Electron. Mater.* **2019**, *1*, 2531–2540.
[28] G.-Y. Wu, X.-Q. Wang, L.-J. Chen, Y.-X. Hu, G.-Q. Yin, L. Xu, B. Jiang, H.-B. Yang, *Inorg. Chem.* **2018**, *57*, 15414–15420.
[29] J.-H. Tang, J. Sun, Z.-L. Gong, Z.-Y. Li, Z. Zhou, H. Wang, X. Li, M. L. Saha, Y.-W. Zhong, P. J. Stang, *J. Am. Chem. Soc.* **2018**, *140*, 7723–7729.
[30] Z. Chen, J.-H. Tang, J. Chen, Y. Xu, H. Wang, Z. Zhang, H. Sepehrpour, G.-J. Cheng, X. Li, P. Wang, Y. Sun, P. J. Stang, *Organometallics* **2019**, *38*, 4244–4249.
[31] M. Li, S. Jiang, Z. Zhang, X.-Q. Hao, X. Jiang, H. Yu, P. Wang, B. Xu, M. Wang, W. Tian, *CCS* **2020**, *2*, 337–348.
[32] M.-L. He, S. Wu, J. He, Z. Abliz, L. Xu, *RSC Adv.* **2014**, *4*, 2605–2608.
[33] S. Yadav, P. Kannan, G. Qiu, *Org. Chem. Front.* **2020**, *7*, 2842–2872.
[34] A. Mallick, A. M. El-Zohry, O. Shekhah, J. Yin, J. Jia, H. Aggarwal, A.-H. Emwas, O. F. Mohammed, M. Eddaoudi, *J. Am. Chem. Soc.* **2019**, *141*, 7245–7249.
[35] X. Chang, Z. Zhou, C. Shang, G. Wang, Z. Wang, Y. Qi, Z.-Y. Li, H. Wang, L. Cao, X. Li, Y. Fang, P. J. Stang, *J. Am. Chem. Soc.* **2019**, *141*, 1757–1765.
[36] G. G. Huang, C.-J. Lee, J. Yang, Z.-Z. Lu, M. Sathiyendiran, C.-Y. Huang, Y.-C. Kao, G.-H. Lee, K.-L. Lu, *Sens. Actuators B* **2018**, *254*, 424–430.
[37] S. K. Kannan, B. Ambrose, S. Sudalaimani, M. Pandiaraj, K. Giribabu, M. Kathiresan, *Anal. Methods* **2020**, *12*, 3438–3453.
[38] Z. Lin, M. Wu, M. Schäferling, O. S. Wolfbeis, *Angew. Chem. Int. Ed.* **2004**, *43*, 1735–1738; *Angew. Chem.* **2004**, *116*, 1767–1770.
[39] V. Vajpayee, Y. H. Song, M. H. Lee, H. Kim, M. Wang, P. J. Stang, K.-W. Chi, *Chem. Eur. J.* **2011**, *17*, 7837–7844.
[40] Z. Zhou, D.-G. Chen, M. L. Saha, H. Wang, X. Li, P.-T. Chou, P. J. Stang, *J. Am. Chem. Soc.* **2019**, *141*, 5535–5543.
[41] Y. Zhou, Z. Xu, J. Yoon, *Chem. Soc. Rev.* **2011**, *40*, 2222–2235.
[42] Y. Liu, X. Wu, C. He, R. Zhang, C. Duan, *Dalton Trans.* **2008**, 5866–5868.
[43] H. Wu, C. He, Z. Lin, Y. Liu, C. Duan, *Inorg. Chem.* **2009**, *48*, 408–410.
[44] Y. Liu, X. Wu, C. He, Z. Li, C. Duan, *Dalton Trans.* **2010**, *39*, 7727–7732.
[45] A. J. Plajer, E. G. Percástegui, M. Santella, F. J. Rizzuto, Q. Gan, B. W. Laursen, J. R. Nitschke, *Angew. Chem. Int. Ed.* **2019**, *58*, 4200–4204.
[46] A. Oleksi, A. G. Blanco, R. Boer, I. Usón, J. Aymamí, A. Rodger, M. J. Hannon, M. Coll, *Angew. Chem. Int. Ed.* **2006**, *45*, 1227–1231; *Angew. Chem.* **2006**, *118*, 1249–1253.
[47] J. Malina, M. J. Hannon, V. Brabec, *Chem. Eur. J.* **2007**, *13*, 3871–3877.
[48] L. Cerasino, M. J. Hannon, E. Sletten, *Inorg. Chem.* **2007**, *46*, 6245–6251.
[49] J. Malina, P. Scott, V. Brabec, *Nucleic Acids Res.* **2015**, *43*, 5297–5306.
[50] J. Zhu, C. J. E. Haynes, M. Kieffer, J. L. Greenfield, R. D. Greenhalgh, J. R. Nitschke, U. F. Keyser, *J. Am. Chem. Soc.* **2019**, *141*, 11358–11362.
[51] C. He, J. Wang, P. Wu, L. Jia, Y. Bai, Z. Zhang, C. Duan, *Chem. Commun.* **2012**, *48*, 11880–11882.
[52] P. P. Neelakandan, A. Jiménez, J. R. Nitschke, *Chem. Sci.* **2014**, *5*, 908–915.
[53] M. Zhang, M. L. Saha, M. Wang, Z. Zhou, B. Song, C. Lu, X. Yan, X. Li, F. Huang, S. Yin, P. J. Stang, *J. Am. Chem. Soc.* **2017**, *139*, 5067–5074.
[54] Y. Zhou, J. Yoon, *Chem. Soc. Rev.* **2012**, *41*, 52–67.
[55] A. Mishra, S. Ravikumar, Y. H. Song, N. S. Prabhu, H. Kim, S. H. Hong, S. Cheon, J. Noh, K.-W. Chi, *Dalton Trans.* **2014**, *43*, 6032–6040.

[56] L. E. H. Paul, B. Therrien, J. Furrer, *Org. Biomol. Chem.* **2015**, *13*, 946–953.
[57] Y. Tian, X. Yan, M. L. Saha, Z. Niu, P. J. Stang, *J. Am. Chem. Soc.* **2016**, *138*, 12033–12036.
[58] J. Yoon, A. W. Czarnik, *J. Am. Chem. Soc.* **1992**, *114*, 5874–5875.
[59] a) A. P. Davis, *Chem. Soc. Rev.* **2020**, *49*, 2531–2545; b) X. Sun, T. D. James, *Chem. Rev.* **2015**, *115*, 8001–8037.
[60] C. He, Z. Lin, Z. He, C. Duan, C. Xu, Z. Wang, C. Yan, *Angew. Chem. Int. Ed.* **2008**, *47*, 877–881; *Angew. Chem.* **2008**, *120*, 891–895.
[61] L.-J. Chen, Y.-Y. Ren, N.-W. Wu, B. Sun, J.-Q. Ma, L. Zhang, H. Tan, M. Liu, X. Li, H.-B. Yang, *J. Am. Chem. Soc.* **2015**, *137*, 11725–11735.
[62] a) S. J. Lee, W. Lin, *J. Am. Chem. Soc.* **2002**, *124*, 4554–4555; b) W. Zuo, Z. Huang, Y. Zhao, W. Xu, Z. Liu, X.-J. Yang, C. Jia, B. Wu, *Chem. Commun.* **2018**, *54*, 7378–7381.
[63] J. Dong, C. Tan, K. Zhang, Y. Liu, P. J. Low, J. Jiang, Y. Cui, *J. Am. Chem. Soc.* **2017**, *139*, 1554–1564.
[64] J. Mendez-Arroyo, A. I. d'Aquino, A. B. Chinen, Y. D. Manraj, C. A. Mirkin, *J. Am. Chem. Soc.* **2017**, *139*, 1368–1371.

[65] J. Wang, C. He, P. Wu, J. Wang, C. Duan, *J. Am. Chem. Soc.* **2011**, *133*, 12402–12405.
[66] S. Shanmugaraju, D. Umadevi, L. M. González-Barcia, J. M. Delente, K. Byrne, W. Schmitt, G. W. Watson, T. Gunnlaugsson, *Chem. Commun.* **2019**, *55*, 12140–12143.
[67] B. Jiang, J. Zhang, J.-Q. Ma, W. Zheng, L.-J. Chen, B. Sun, C. Li, B.-W. Hu, H. Tan, X. Li, H.-B. Yang, *J. Am. Chem. Soc.* **2016**, *138*, 738–741.
[68] Z. Li, X. Yan, F. Huang, H. Sepehrpour, P. J. Stang, *Org. Lett.* **2017**, *19*, 5728–5731.